Environmental embrittlement of austempered ductile iron (ADI) – A review

R.E. Boeri[1], R.A. Martínez[1*]

[1]División Metalurgia, Facultad de Ingeniería, Universidad Nacional de Mar del Plata,
INTEMA – CONICET, Mar del Plata, Argentina

In this article, the authors revise the advances in the understanding and characterization of the unusual embrittlement phenomenon. The phenomenon affects the behavior of austempered ductile iron (ADI) while stressed in contact with water and other liquids, reducing its strength, elongation and fracture toughness.

The different investigations carried out by the authors include the characterization of the embrittlement by means of tensile, fracture toughness and cyclic load tests taking into account the influence of selected liquids. The use of electrochemical potentials during testing and the surface protection by different coatings are also discussed.

These results show that there have been significant advances in the characterization of the embrittlement phenomenon since it was first reported.

Based on the examination of the fracture surfaces, a fracture model, called "Localized slip process induced by adsorption in aqueous environments" is proposed.

Introduction

The family of ductile cast alloys (DI) can show different matrix microstructures and can cover a wide range of mechanical properties. As an example, ferritic matrices are used in parts, such as automotive suspension components, where high impact strength is the main requirement. On the other hand, pearlitic and martensitic matrices are used when hardness, strength and wear resistance represent a major issue.

DI production has maintained a sustained rate of growth over the last decades substituting cast and forged steels in a large number of applications. At present, researchers and producers are developing new applications for DI, and targeting the market of safety critical parts when combinations of strength and toughness are required.

The strength of nodular graphite ductile iron increases after an austempering heat treatment process, obtaining the so-called austempered ductile iron (ADI). The microstructure of the resulting matrix is a combination of acicular ferrite and high carbon austenite, also known as ausferrite.

However, ADI suffers a noticeable embrittlement when its surface is in contact with liquids during slow monotonic tensile load application [1-7]. The first reports of embrittlement by contact with water were published by Shibutani et al [1,2]. Martínez et al [3] verified the existence of the phenomenon when obtaining similar results after testing several ADI grades (ASTM A 807M-06). Such studies showed that reductions in tensile strength and elongation could reach 30% and 70%, respectively.The origin of embrittlement remains to be comprehensively unexplained. Nevertheless, the presence of this effect has not stopped the increasing application of ADI in the construction of high strength mechanical components. The very low incidence of brittle failure of ADI in service could be explained by two distinctive characteristics of this effect: it is fully reverted after the part surface is dried, and it is unnoticed at high loading rates. As a result, failure in service requires a relatively slow overloading (initial stages of plastic deformation) when the part is in contact with liquids, which does not occur very frequently.

Embrittlement phenomena by contact with liquids are not unusual. In some cases different groups of materials that regularly have a ductile behavior, among which some metallic alloys are included, show lower ductility and strength when their surfaces are in contact with a specific liquid while stressed over the yield limit. The fracture surface characteristics change from those observed when testing the same material in air [3].

A brief review of the most extensively studied environmentally induced cracking (EIC) processes for this kind of phenomenon includes hydrogen embrittlement (HE), together with stress corrosion cracking (SCC) and liquid metal embrittlement (LME)[10-12]. EIC process is characterized by brittle failures in which cracks propagate at stress intensity (K) levels lower than the critical values in air or vacuum, because of the combined effect of a tensile stress field and the presence of a corrosive media. Corrosion rates are usually quite low. The mechanisms involved in this type of failure are very complex and remain under discussion. In consequence, the occurrence of EIC failures in service is still difficult to predict.

LME causes the catastrophic brittle failure of normally ductile metal alloys in contact with a liquid metal and stressed in tension[13]. The fracture mode changes from a ductile to a brittle intergranular or brittle transgranular

---

(cleavage) mode. It has been shown that the stress needed to propagate a sharp crack or a flaw in liquid is significantly lower than that necessary to initiate a crack in the liquid metal environment. In most cases, the initiation and the propagation of cracks appear to occur instantaneously, with the fracture propagating through the entire test specimen. The velocity of crack or fracture propagation has been estimated to be 10 to 100 cm/s. LME is not a corrosion, dissolution or diffusion–controlled intergranular penetration process. The embrittlement is severe, and the propagation of fracture is very fast in the case of LME as compared to that in SCC.

The authors have studied the embrittlement of ADI over the last years. The general features of this embrittlement shares some common features with LME. The objective of this manuscrip is to present a critical review of the general features of ADI embrittlement and to introduce some recent results about the influence of cyclic loading.

Experimental Procedure

Several ductile cast iron melts were prepared in a medium frequency induction furnace. Steel scrap and foundry returns were used as raw materials. Nodulization was carried out using the sandwich method with 1.5 Wt% of Fe-Si-Mg (6% Mg) and inoculated with 0.6 Wt% Fe-Si (75% Si). The chemical compositions of the melts were determined by using a Baird DV6 spectrometer. (Table 1).

Table 1: Chemical composition of the melts.

Melt	C	Si	Mn	Mg	Cu	Ni	Mo	P	S
A	3.20	3.30	0.2	0.03	1.00	0.68	0.09	0.01	0.01
B	3.35	2.74	0.32	0.062	1.05	0.44	---	0.02	0.01
C	3.32	1.77	0.18	0.05	0.06	---	---	0.06	0.02
D	3.20	3.30	0.2	0.03	1.00	0.68	0.09	0.01	0.01
E	3.58	1.95	0.18	0.046	1.08	0.38	0.18	0.02	<0.01
F	3.45	2.3	0.25	0.65	---	---	---	0.01	<0.01

One inch "Y" blocks were cast in sand molds and used to prepare different specimens such as those shown in Fig. 1.
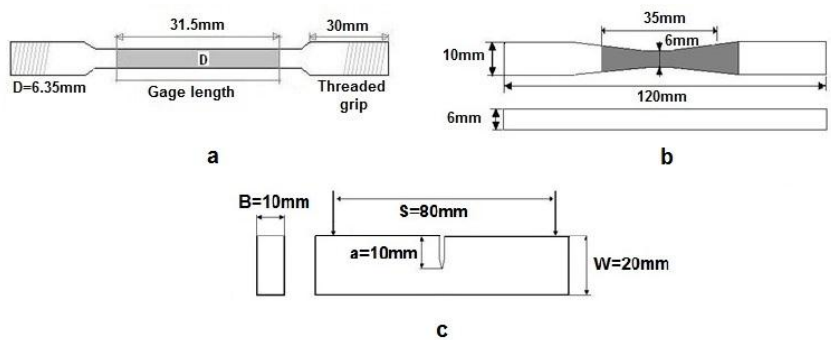
Fig.1: Samples used for mechanical tests

The experimental setups used to carry on the tests in wet condition are shown in Fig. 2 a and b. The first shows the arrangement in the case of tensile test using samples such as shown in 1a and 1b, the second is a sketch of the double eccentricity machine used to apply cyclic loads to samples SEN(B) /ASTM E399). This machine, producing a displacement-controlled cyclic load, was used with a constant eccentricity $e = 0.145$ mm, which resulted in stable crack propagation under small-scale plasticity condition.
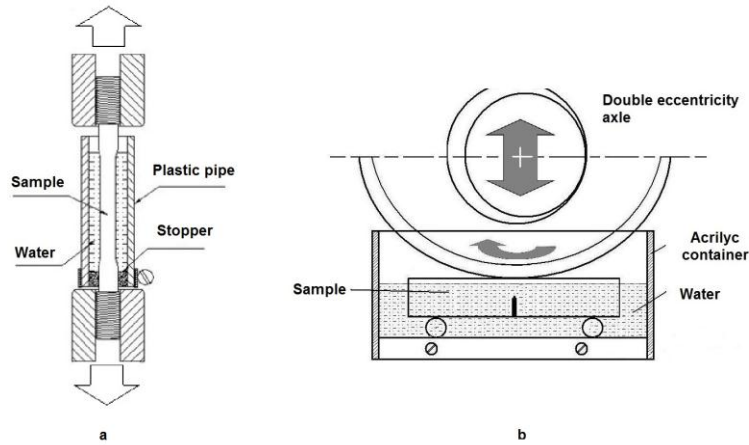
Fig.2: Experimetal set up used for wet tensile and cyclic load tests

Test samples of the different melts were heat treated to obtain different ADI grades. The heat treatments applied to each melt are detailed in Table 2.

Results and Discussion

1. Tensile tests
1a. Different ADI grades
Table 2 lists the results of tensile testing of samples of melt A of different ADI grades. In all cases, significant drops in UTS and elongation are caused by the presence of water in contact with the surface of the sample.

Table 2: Tensile tests

Material		U.T.S.[MPa]/δ[%]	Heat tretment
ADI 150-110-7 (grade 2)	Dry	1168/16	60´@900ºC+90@360ºC, air cooling
	Wet	852/2.8	
ADI 175-125-4 (grade 3)	Dry	1340/11.3	60´@910ºC+90@320ºC, air cooling
	Wet	1030/3	
ADI 200-155-2 (grade 4)	Dry	1526/6.3	60´@910ºC+90@280ºC, air cooling
	Wet	1071/1.2	
Ferritic matrix	Dry	517/25	24hs@680ºC, furnace cooling
	Wet	516/26	
Pearlitic matrix	Dry	1100/7.3	60´@910ºC , air cooling
	Wet	900/3.1	

Melt A (Table 1), sample a (Fig. 1), ADI standard ASTM A 897-06

1b. Crack develoment
The process of cracking and failure under tensile stresses has been studied by the metallographic inspection of the polished and etched surfaces of the samples shown in Fig. 1-b. A careful inspection of the samples showed that above certain stress levels, cracking begins at certain locations of the microstructure, as shown in Fig. 3
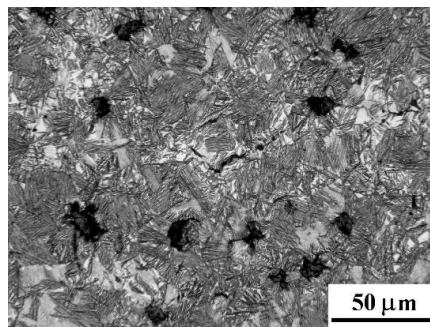
Fig.3: Crack developed in LTF zone after small plastic deformation.

A careful analysis of the location of the first cracks showed that they form at some specific portions of the microstructure usually called <u>L</u>ast <u>T</u>o <u>F</u>reeze (LTF). LTF distribution and chemical composition are the result of the solidification process. The solidification of spheroidal graphite iron involves the nucleation and growth of relatively large austenite dendrites. The microsegregation of the alloy elements takes place between the dendrite arms, therefore, the distribution of the LTF regions is intradendritic and its dispersion depends on the dendrite coarseness. Given the fact that LTF zones solidify at the end of the process, they can show a higher or lower concentration of some alloy elements and impurities as well as small shrinkage cavities [6,7]. The chemical composition of DI always includes Mg, C, Mn, Si, S, and P; while elements like Mo, Cu, and Ni are frequently added as alloying elements. Therefore, LTF regions can show varied chemical compositions and properties for different ductile iron alloys. In general terms, the higher the alloying content, the larger the microsegregation. Hence, the ADI fracture process should be analyzed on a material that can be considered to be formed by an ausferritic metallic matrix that shows spherical cavities of different sizes (the strength of the graphite occupying these sites is negligible), and certain sites in the matrix (LTFs) where microporosity, non-metallic inclusions and phases such as phosphides, carbides etc. may be present. Indeed these zones present adverse characteristics from a mechanical properties viewpoint.

1c Influence of Different liquids
The presence of water in contact with the surface of the samples causes the formation of surface cracks at lower stress levels. A stress level above 850 Mpa, barely larger than the yield strength, is enough to begin cracking in the presence of water. Other liquids show similar behavior to that of water, but induce higher critical cracking stress [9]. The influence of liquids on the surface crack initiation was determined by using the samples shown in Fig. 1b. Those samples allow investigating the surface integrity after a given stress or strain has been applied. Fig. 4 shows the stress threshold for the formation of cracks determined for the different liquids used. It is very clear that the presence of the liquids facilitates the initiation of surface cracks.
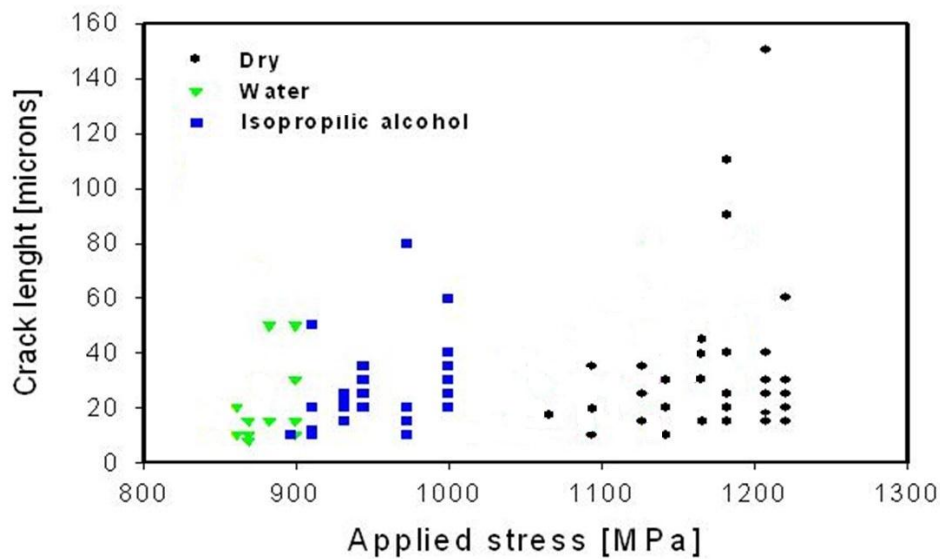
Fig.4: Crack development using different liquids. Melt B. Sample b. ADI grade 2

The obtained threshold values results are summarized in Table 3.

Table 3: Crack initiation threshold values.

Media	Air	Heptane	Ethanol	CCl₄	Water	Isopropyl alcohol
Threshold stress [MPa]	1020	910	903	923	851	880

Melt B. Sample b, ADI grade 2.

In addition, Different liquids cause different degrees of embrittlement. The degree of embrittlement could not be clearly related neither to polarity, nor to surface tension.

2. Fracture toughness and hardness

The fracture toughness tests were performed using blunt notched (BN) and precracked (P) samples. The results are listed in Table 4. For both stress concentrators, the values of K_{IC} in wet condition were nearly half of the values obtained when the samples were tested in dry condition. The critical flaw size is also calculated and displayed in the table.

Table 4: Fracture toughness

Sample	Condition	K_{IC} [MPa.m$^{1/2}$]	$\{K_{IC}/\sigma_{YS}\}^2$ [mm]
BN	Dry	72.5	0.6
BN	Wet	34.2	0.15
P	Dry	53.4	0.36
P	Wet	26.8	0.09

Melt C, sample c.ADI grade 2

The hardness measurements show small but consistent changes because of wetting. The hardness of ADI Grade 2 of melt C measured in dry condition reaches 318HB, while it increases to 335HB when the tests are carried out in contact with water. These results suggest that the strain hardening increases when the surface of the ADI is wet.

The observation of the inner surface of the hardness test indentation by optical microscopy showed a flat surface with signs of plastic deformation and scratches produced by the friction between the ball and the material when the measurement was done in dry condition. On the other hand, the inner surface of the indentation when the test was carried out on samples submerged in water showed a very different aspect including striations, which contain small cracks observable at high magnification, and preferentially located at cellular boundaries (LTF zones).

3. Cyclic loads

The behavior of samples tested after applying cyclic loads to samples a of melt C on ADI Grade 2 is summarized in Fig. 5 where the crack length is plotted against test time and number of cycles. It can be noticed that cracks nucleate earlier in submerged samples than in samples tested in dry condition, and also that the crack growth rate is greater for the submerged samples, as shown by the slope of the curves.
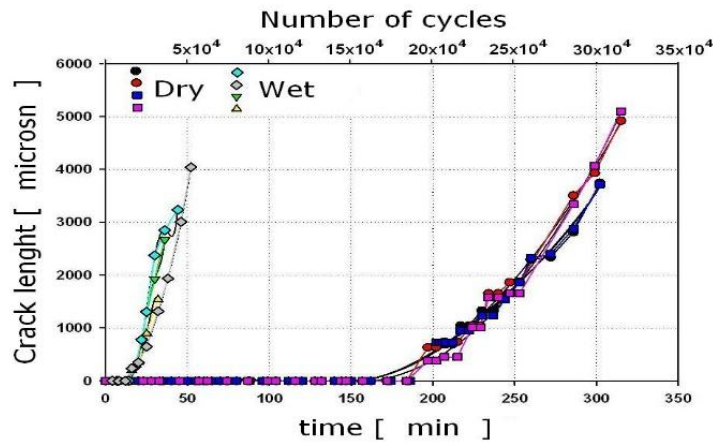
Fig. 5: crack length as a function of test time and number of cycles.

The values measured for nucleation time and growth rate showed very low dispersion. The results shows that the application of cyclic loads under wet conditions severely affects the fatigue resistance of ADI, facilitating the nucleation of cracks and increasing the fatigue crack growth rate.

4. Influence of testing under controlled electrochemical potential

The application of controlled potential during tensile testing of ADI in contact with water neither enhances nor inhibits the embrittlement effect observed under free potential testing conditions, as shown by the results listed on Table 6. This has been the case for both anodic and cathodic conditions. This result supports the hypothesis that H atoms are not responsible for the embrittlement.

Table 5: Results of tensile testing of ADI under free and controlled electrochemical potential.

Test condition	U.T.S.[MPa]	Elongation %
E_{CORR}=-0.69/-0.72(SCE)	863	3
Wet cathodic potential=1.45V(SCE)	857	3
Wet anodic potential=-0.55V(SCE)	868	3
Dry	1168	16

Melt D. Sample a. ADI grade 2

These result were also supported by tests performed by Caballero et al. [7]

5. Efficiency of protective coatings.

Despite the apparent lack of practical incidence of the embrittlement effect, the identification of technical means to alleviate its influence is highly desirable. A first look into the problem would indicate the convenience of painting or coating the surface of ADI parts to isolate it from the environment. The ability of different paints and metallic coatings to protect ADI against embrittlement by contact with liquids has been examined experimentally. The results are listed in Table 7. Only an acrylic coating reinforced by fibers worked against embrittlement. It is apparent that for a coating to be effective, it must be able to withstand relatively large elastic deformations. The protection is effective only when the surface layer integrity is not affected by the deformation undergone by the substrate, and then, the contact of water with ADI surface is prevented. Additionally, the efficiency of a water repellent agent was tested. After spraying the samples with WD40 ®, they were submerged in water and tested. No signs of embrittlement were observed.

Table 6

Sample ID/test condition	U.T.S. [MPa]	δ [%]
Uncoated/Dry	1050	14.8
ASTM 897M-06	900	9
Uncoated/Wet	843	1.2
H-Epoxy/Wet	837	1.4
S-Epoxy/Wet	873	3
Polyester/Wet	823	3.4
Polyester-U/Wet	807	4
E-Zinc/wet	817	1.3
M-Zinc/wet	833	2.8
E-Tin/Wet	795	3.3
Acrilyc w/fibers/Wet	1010	13.8
WD40®/Wet	1040	14.6

Melt E. Sample a. ADI grade 2

6. Influence of Chemical Composition and fracture model
Evaluation on unalloyed samples

Since, as discussed in section 1-b, LTF zones are the main spots for crack initiation when the material is loaded, it is important to assess the influence of the characteristics of the LTF zones on the embrittlement of ADI. With this aim, grade 2 ADI samples of the unalloyed Melt F, which show very low microsegregation at the LTF, were tested in wet conditions, resulting in drops of 15% in UTS and 80% in elongation, while yield stress remained at the same level. As opposed to what was hypothesized, the use of non-alloyed ductile iron with minimized LTF zones neither inhibited nor reduced the embrittlement phenomenon.

The microscopical study of the lateral surface after loading the samples at higher magnification reported nucleation and growth of cracks in LTF zones. These observations demonstrate that the initiation of cracks in unalloyed DI proceeds in the same manner as that previously verified in low alloy DI, thereby indicating that suppressing the alloy elements in the melt does not improve the strength of LTF zones nor prevents crack initiation.

Fracture mechanism model

It has been shown that microsegregated regions of the ADI microstructure, usually referred to as Last To Freeze (LTF), cracked during testing after plastic deformation starts, acting as initiation sites of the embrittlement process (Fig. 3).

The ductile fracture process is sketched in Fig. 6a, where the classic mechanism of growth and coalescence of voids opperate in nodule cavities and inclusion possibly located at LTF.

A different mechanism is proposed for liquid submerged samples (Fig. 6b). In this case, the first few atomic layers at the crack tip adsorb water molecules that weaken the metal interatomic bonds and facilitate the dislocation nucleation. Alternated dislocation injection from the crack tip on planes D1 and D2 produces a crack tip growth Δa. New voids

generation produce further crack growing by alternate slip coalescence. In this manner, the macroscopic fracture bisects the active slip planes.

Compared with the ductile process less blunting occurs at crack tip, strains ahead of crack tip are lower and voids form only just ahead of cracks. Therefore, the fracture surface displays small shallow dimples as shown in Fig 6b.
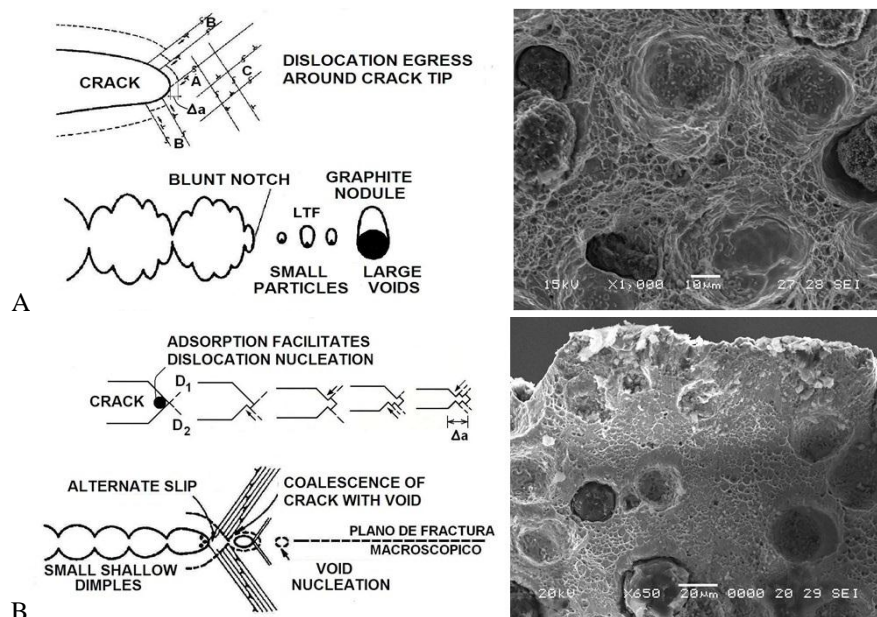
Fig.6: Ductile growth (A) and water assisted growth (B).

The fracture surface of a sample submerged is shown in Fig. 7. The enclosed area at the top is the zone where the crack started to grow with water assistance. It is shown that after reaching a critical size the fracture continues with the ductile mechanism (area outside the white line).
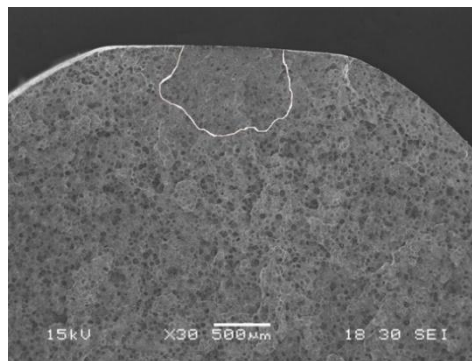
Fig.7: Fracture surface of a tensile sample.

Final Remarks

The research on the embrittlement of ADI over the last years has proven that:

1. Significant drops in UTS and elongation are caused by the presence of water and other liquids in contact with the surface of the sample. Different liquids cause dissimilar degrees of embrittlement.
2. The presence of liquids facilitates the initiation of surface cracks. Cracks nucleate at the microsegregated last to freeze portions of the metal matrix.
3. The presence of water on the surface of ADI causes also drops on fracture toughness and increase of hardness values.
4. The application of cyclic loads under wet conditions severely affects the fatigue resistance of ADI, facilitating the nucleation of cracks and increasing the crack growth rate.
5. The strategy of protecting the surface by coatings to avoid embrittlement is effective only when the integrity of the coating surface layer is not affected by the deformation undergone by the substrate, and then, the contact of water with ADI surface is prevented.
6. The amount of alloy elements present in the alloy does not influence the embrittlement degree of ADI, i.e., a stronger microsegregation at the LTFs does not affect the amount of embrittlement.

References

1. S. Komatsu; C.Q .Zhou; S. Shibutani; Y Tanaka, Int. J. Cast Metals Res., **11,** 1999. p. 539-544
2. S Komatsu, Y. Osafune, Y. Tanaka, K. Tanigawa, S. Shibutani, H. Kyogoku, Int. J. Cast Metals Res. **16**, 2003 p. 209-214
3. R. A. Martínez, R. E Boeri, J. A Sikora,, Int. J. Cast Metals Res., **13,** 2000 p. 9-15
4. R. A. Martínez, S. N. Simison and R. E. Boeri, 2002 World Conference on ADI, pp. 91-96, 26-27 September 2002, Louisville, KY. USA
5. *R. A. Martínez, S.N. Simison and R .E. Boeri, Int. J Cast Metals Rev. 2003 Vol. 16 no. 1-3, pp. 251-256*
6. *L. Masud, R. A. Martínez, S. Simison and R. E. Boeri ,Journal of Material Science.38 (2003) 2971-2977*
7. L. Caballero, M Elices and R.N. Parkins. Corrosion. Vol. 61, No.1. 2005 pp. 51-57
8. B. Daga, R. A. Martínez, S. Simison, R. E. Boeri, Annals of the Seminar SAM / CONAMET Congress/ MATERIA Symposium 2003, San Carlos de Bariloche, Argentina. pp. 647-650
9. B. Laine, S. N. Simison, R. A. Martínez, R. E. Boeri, Annals of the Congress CONAMET/ SAM – SIMPOSIO MATERIA 2002, Santiago de Chile, Chile. pp. 121-126
10. T. Lemme, R. A. Martínez, S. N.- Simison, R. E. Boeri, Conference SAM –CONAMET 2004, La Serena, Chile. pp. 457-462
11. *R E. Boeri; R A. Martínez; Materials Science and Technology, Volume 29, Number 6, June 2013 , pp. 665-671(7)*
12. R.A. Martinez ,Engineering Fracture Mechanics 77 (2010) 2749–2762
13. P. Zanotti, S. Simison, R. A. Martínez, R. E. Boeri, Annals of the Binational Congress SAM/CONAMET 2005, Mar del Plata, Argentina. ISBN 987-2243-0-8
14. S. Lynch, Mater. Forum, 11, 268-283, 1988.
15. Anderson, T. L. (1994) Fracture Mechanics. Fundamentals and Applications. Chapter 12. 2nd edition, CRC Press; Boca Raton, Florida, USA. (book)